SINGLE-CAMERA SYSTEM FOR MEASURING PAPER DEFORMATIONS BASED ON IMAGE ANALYSIS

Paweł Pełczyński, Włodzimierz Szewczyk, Maria Bieńkowska

Centre of Papermaking and Printing, Lodz University of Technology, 90-924 Lodz, Wolczanska 223, Poland,
(✉ *pawel.pelczynski@p.lodz.pl,* +48 42 631 38 16, *wlodzimierz.szewczyk@p.lodz.pl, maria.bienkowska@p.lodz.pl*)

Abstract

The article presents a new technique for measuring paper deformation in unidirectional tensile tests, based on recording and analysis of a series of specimen images. The proposed technique differs from the DIC-based deformation measurement in that the cross-correlation of image data has been replaced with linear filtering. For this purpose, a regular grid of markers is printed on the sample. Filtering the image creates local maxima in the places where markers occur. The developed algorithm finds their location with sub-pixel accuracy. Printing a grid of markers on tested paper and use of reference objects visible in the same image as the paper sample, freed from the need to mechanically connect the camera and the universal testing machine and from the necessity to electronically synchronize their work. The obtained deformation distributions and Poisson's ratios are in accordance with the literature data which confirms the correctness of the developed measurement technique.

Keywords: digital image processing, characteristic point tracking, paper physical properties, deformation analysis, Poisson's ratio.

1. Introduction

Machine-made papers show distributions of mechanical properties characteristic of anisotropic bodies. Measurements of these properties are usually performed in two main directions of orthotropics in the paper plane. The first of these is the direction of paper web production on a paper machine, called *machine direction* (MD). The second one is the *cross direction*, perpendicular to the machine direction and designated as CD. The basic test of mechanical properties of paper, which is the unidirectional tensile test (PN-EN ISO 1924-2:2010 standard), provides a lot of information about the tested material and allows to determine such properties as *e.g.* deformation at break, breaking force, Young's modulus, energy absorbed at breaking [1]. Most often, tensile tests are carried out using material *universal testing machines* (UTM). Commonly used machines of this type allow for registration of changes in force and deformation in the tensile direction, but they do not provide the ability to measure deformation in a direction perpendicular to the tensile

direction. The deformation measurement of the tested material is carried out by measuring the displacement of the moving handle of the testing machine. For this reason, its accuracy can be significantly reduced by sliding the stretched material out of the jaws as well as by disrupting the unidirectional state of stress through the jaws, blocking the transverse deformation of the stretched material where the sample is held. Based on the measurement made by the testing machine, an average deformation value is obtained and it is not possible to register its local value in different areas of the sample under test.

All these inconveniences can be avoided by using non-contact optical deformation measurement. Non-contact measurement methods include measurements based on the registration and analysis of images of samples under tension. A comprehensive review of the applications of image analysis -based methods in solid mechanics can be found in [2]. They are usually based on registering a series of images of samples subjected to force by a stationary camera rigidly mounted in the measuring system or by a stereoscopic camera system [3]. The images are digitally undistorted, rectified and other required pre-processing operations are performed. Then subsequent images in the registered sequence are compared with each other to estimate the displacement of surface elements of the material being tested. The most common technique for estimating displacements is determining the local cross-correlation of image data and estimating the location of its maximum. The technique is called *Digital Image Correlation* (DIC) and it was successfully used in deformation analysis [4–6]. Its advantage is the possibility of estimating displacements with sub-pixel accuracy [7]. It is particularly desirable in the task of determining surface deformations measured as differences in displacement of the sample surface fragments related to the distance between them. This technique has been successfully used in methods of determining the movement of liquid and gas particles called *Particle Image Velocimetry* (PIV) and deformations generated in various materials under the influence of applied forces [8,9]. The wide range of applications of the displacement and deformation image analysis contributes to the emergence of more and more advanced DIC varieties, an example of which is the GeoPIV-RG (Reliability Guided) algorithm published in [10]. The achieved accuracy in determining image translation with this algorithm is at the level of 2×10^{-3} pixels. A group of image analysis methods based on determining optical flow is also gaining more and more popularity in studies of material deformations [11,12] despite the limitations of this approach which are mainly due to the limited range of displacements [13].

The necessary condition for obtaining good measurement resolution and its high accuracy in the methods mentioned above is the presence of texture on the surface of the tested materials [14]. If the surface has no natural texture, irregular patterns are usually applied to it. The technique of spraying matte paints or other adhesive sprays that leave a pattern with the highest possible contrast, is commonly used. An example of this approach is testing materials using GOM's ARAMIS optical measuring system. Unfortunately, not all materials tolerate this technique, a good example of which is paper. Solvents contained in paints may change its mechanical properties. In this situation, the test is usually limited to observing the edges of samples or markers stuck to their surface. An example here may be the video Xtens 2-120 HP optical extensometer by Zwick Roell [15]. Both these deformation testing systems are based on a stereoscopic system of rigidly connected digital cameras. One requires calibration using a calibration object specially prepared by the manufacturer to achieve the assumed measurement accuracy, and the other requires rigid attachment to the testing machines.

The problems encountered when examining paper deformations with optical methods and the high prices of commercial systems for performing such tests prompted the authors to develop a system for deformation measurement which is dedicated to testing paper products.

2. A new technique for measuring deformations

In order to measure deformations in the paper plane in various directions, a measuring technique based on image analysis methods was developed. It allows for analysis of average deformation values of the entire examined area as well as the distribution of deformations in selected fragments. Its main assumption is non-contact measurement of deformation of paper samples by analysing a series of high-resolution images registered during stretching of sample in a testing machine. To enable tracking of paper deformations, a regular dot pattern was printed on its surface in a 1 mm square grid similarly to [16]. In most systems a regular pattern cannot be used due to the risk of incorrect matching of subsequent images of the examined object. In the discussed system, thanks to the development of a new marker tracking algorithm, this is not a problem. The use of a known pattern also allows finding camera position parameters relative to the tested sample and eliminating errors resulting from inaccuracy of its positioning. It was also checked that printing a pattern of dots with a laser printer does not cause measurable changes in the mechanical properties of the paper.

A measurement setup was designed and software was developed in the form of a script and function package for processing and analysing recorded images in the GNU Octave – mathematical modelling environment. The unique features of the proposed measurement technique are:
- commonly used cross-correlation of image data for surface motion tracking has been replaced with linear filtering featuring a lower computational cost,
- printing a grid of markers on the tested paper and the use of reference objects visible in the same image as the paper sample, freed from the need to mechanically connect the camera and universal testing machine and from the necessity to electronically synchronize their work.

2.1. Measuring stand

Due to the wide range of measurements of the mechanical properties of paper, it is not possible to determine the precise requirements for the dimensions of the field under examination in advance, which was the reason for the decision to use a mobile image capture system equipped with a camera with interchangeable optics. The measuring stand (Fig. 1a) consists of a Zwick Roell Z020 testing machine, a Canon EOS 6D Mark II full-frame DSLR camera with Canon MP-E 65 mm f/2.8 1–5× Macro lens placed on a camera tripod and an illuminator ensuring
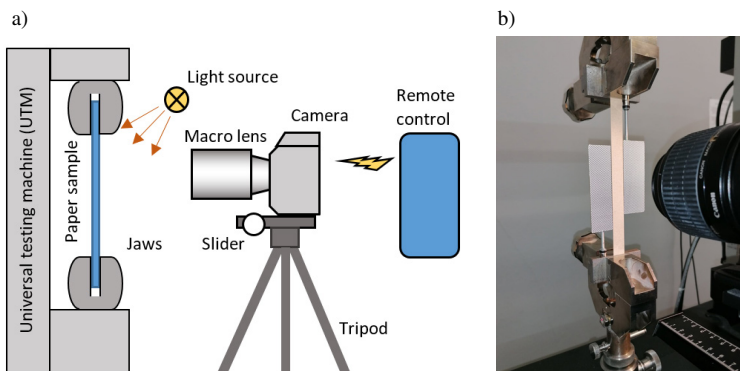

Fig. 1. a) Measurement stand, a) overall concept, b) view of main parts of a stand.

constant illumination. Macro lens gave the opportunity to focus on measuring local deformations and assessing their heterogeneity.

In order to ensure image sharpness adjustment, the camera is attached to a tripod with the possibility of adjusting the position in two horizontal axes – parallel and perpendicular to the camera's optical axis. The camera lens allows manual change of the projection scale in the range of 1 to 5 which gives the size of the observed fragment of the paper sample in the range of 7.2×5.8 mm to 36×24 mm. The camera has a 26.2-megapixel CMOS image sensor with a distance between pixels of 5.73 μm, and the size of the recorded images is 6240×4160 pixels. In the early development of imaging techniques CCD cameras were usually used for surface deformation analysis. Recent works [17] show that the progress made in the technology of image sensors based on CMOS technology now allows successful use of this type of cameras. The camera allows to record a series of images initiated from a remote-control unit which eliminates vibrations resulting from pressing the shutter button. The camera is set to the mode of recording series of images, and the image data stream is saved on the memory card. In addition, the camera mirror is permanently raised during registration so that its movement does not introduce vibrations. Images are saved as RAW data to avoid distortions introduced by JPEG compression.

To enable tracking of paper deformations, a regular pattern of small dots is printed on the surface of paper samples using a laser printer. After printing the dot grid (Fig. 1b), the tested paper sample is subjected to air conditioning. Then it is mounted in the jaws of the machine and subjected to the initial force in order to pre-tension it. The camera is set so that its optical axis coincides with the normal to the plane of the paper. The recording of a series of images is initiated before starting the tensile test in order to synchronize the measurement of displacement and force in the testing machine and the results of deformation estimation from image sequence. Registration ends when the measurement is completed.

2.2. Image processing and analysis

The image sequence recorded in the measurement process is subjected to pre-processing and analysis. Individual steps of the image pre-processing and analysis, leading to finding a rectangular dot grid, are shown in Fig. 2 on the example of analysing a small part of a packaging paper sample.
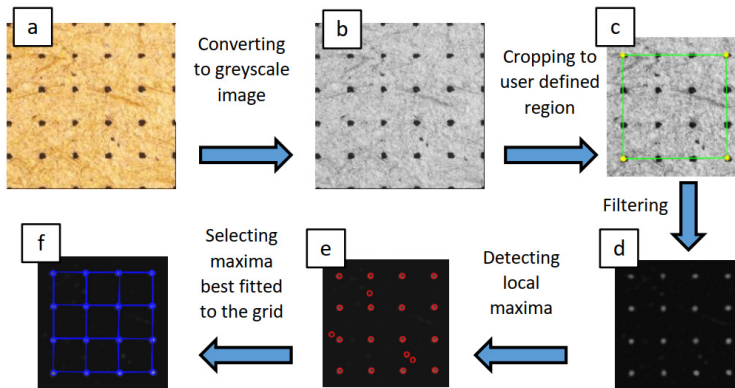

Fig. 2. Stages of image processing and analysis and the resulting images: a) input image, b) greyscale image, c) image cropped to the fragment indicated by the user by selecting markers limiting the area of interest, d) filtered image, e) local maxima projected on the filtered image, f) local maxima best fitted to the theoretical grid in the first image or the previously found grid.

Image data is saved in a three-dimensional array of numbers $M \times N \times 3$, where M – the vertical dimension (number of pixels), N – the horizontal dimension, and 3 denotes the number of the colour component (RGB representation). Image data is normalized to the range [0, 1]. Figure 2a shows a part of the image of the sample surface which is characterized by a brownish colour and natural texture. Unfortunately, it has a low contrast which does not allow for reliable tracking of the sample surface displacements without the use of additional markers. Then the colour image is converted to a greyscale one (Fig. 2b). In order to limit the field of analysis to a rectangular area containing the printed grid of dots, the image coordinates of the vertices of the quadrangle defining the examined area visible in the first image of the sequence are determined (Fig. 2c). In the following sequence of images, the same portion of the image is automatically selected for further processing. Based on horizontal and vertical resolution of the image sensor, the position (x_p, y_p) of each p point of the image is determined:

$$x_p = \frac{j - j_{beg}}{RES_x}; \qquad y_p = \frac{i - i_{beg}}{RES_y}, \tag{1}$$

where:
i, j – the coordinates of the p point in the digital image,
i_{beg}, j_{beg} – digital image coordinates of the origin of the reference system,
RES_x – horizontal resolution of the digital image, pixel/mm,
RES_y – vertical resolution of the digital image, pixel/mm.

The analysis of a paper sample image sequence begins with finding the position of printed dots in the coordinate system defined in the digital image space. For the purpose of dot detection, linear image filtering is used with a specially designed linear filter, the mask of which is shown in Fig. 3a. Linear filtering of a monochrome digital image is defined as the two-dimensional convolution of a matrix representing the image with the filter mask:

$$I_{dot} = I \cdot h, \tag{2}$$

where:
I_{dot} – filtered image,
I – original image,
h – linear filter mask.

The convolution of a image with the mask is by definition an operation similar to the calculation of the cross-correlation of two image fragments which is used in recognized methods of analysing the deformation of the surface of bodies and referred to as DIC [4]. The main difference is the replacement of the reference image which is the first or previous image in the analysed sequence, with the dot model described by the following formula:

$$h(u, v) = \begin{cases} \sin c\left(10 \cdot \dfrac{\sqrt{u^2 + v^2} \cdot \pi}{RES}\right) & \text{for} \quad \sqrt{u^2 + v^2} \leq 0.2 \cdot RES \\ 0 & \text{otherwise} \end{cases}, \tag{3}$$

where:
u, v – coordinates, px,
RES – average value of spatial resolution.

The filter designed in this way is characterized by a strong suppression of local, high-frequency image disturbances and, at the same time, it is insensitive to changes in image brightness due to strong suppression of its frequency response for the DC component (dark spot in the middle

of Fig. 3b. The applied mask maximizes filter response in places where dark dots occur, which gives local maxima in the resulting image (Fig. 2d). The single dot in this image is represented by a smooth, convex surface with the peak at the centre of the dot. Its vertex coordinates are determined with sub-pixel accuracy by matching the model surface described with an elliptic paraboloid, optimizing its equation coefficients by minimizing the mean square error between the real and model surface. Local maxima exceeding the experimentally set threshold are indicated in Fig 2e with red circles. The next step in the analysis is assigning the maxima found to the theoretical square grid of points. Each nod, is assigned the closest maximum found, if its distance is less than half the distance between the nodes. In this way, false maxima not fitted to the grid and those outside of the defined rectangle are discarded. The resulting grid of points is shown in Fig. 2f. The procedure is used only for the first image of the sequence. In subsequent images the local maxima are matched to the already found grid in the previous image. The small displacement of the dots between consecutive images prevents the problem of mis-matching of adjacent markers. Repeating this operation for all images in the sequence allows to track the movement of local fragments of the stretched sample containing printed dots.
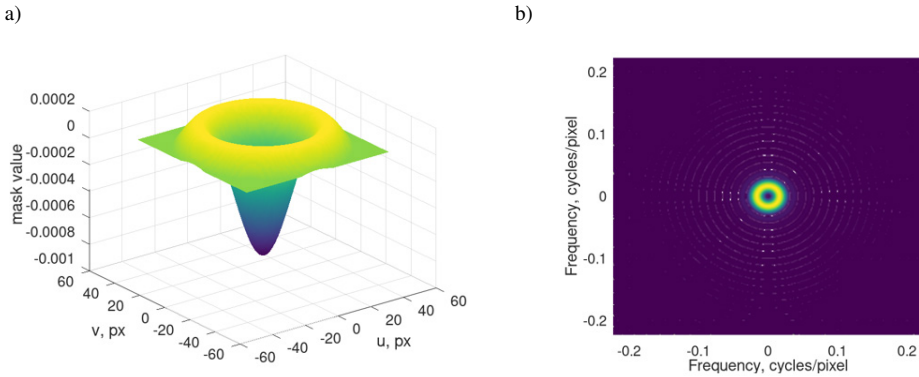

Fig. 3. a) Linear "dot" filter mask, b) 2D frequency response of the designed filter.

As a result of image analysis, the location of dots on the surface of the image sensor is obtained. To be able to determine the position of the dots on the surface of the tested sample, it is necessary to correct the distortions caused by the camera's optical system as well as those resulting from the perspective projection [8]. Thanks to the very good quality of the Canon MP-E 65 macro lens used, very low level of distortions is introduced by its optics, and the image distortion correction step could be omitted. It was assumed that the camera optics meets the pinhole camera model. The problem of removing perspective turned out to be insignificant when using a macro lens which has a very shallow depth of field. Setting the camera in order to ensure good sharpness of the whole image at the same time ensures the perpendicularity of the optical axis to the photographed paper sample. The use of a print of square dot grid provides the information needed to identify scale S of projection and find real coordinates of dot markers on paper specimen:

$$x = \frac{x_p}{S} ; \quad y = \frac{y_p}{S} . \tag{4}$$

2.3. Analysis of measurement data

Further analysis involves operations on the position of dots on the paper surface. The first stage is determining the displacement of regular grid dots (expressed in millimeters) between the first image and image *n* in the sequence according to the relationship:

$$\begin{cases} mx(k, l, n) = x(k, l, n) - x(k, l, 1) \\ my(k, l, n) = y(k, l, n) - y(k, l, 1) \end{cases}, \tag{5}$$

where:
    mx – displacement of dot (k, l) in the *x* coordinate,
    my – displacement of dot (k, l) in the *y* coordinate,
    $k, \ l$ – column and row number in the regular grid to which the given dot belongs.

The next stage of the measurement data analysis is the determination of local deformation in grid point (k, l) defined as the difference of displacements of points located in the grid at positions differing by *m* columns or rows:

$$\begin{cases} \Delta x(k, l, n) = mx(k + m, l, n) - mx(k - m, l, n) \\ \Delta y(k, l, n) = my(k, l + m, n) - my(k, l - m, n) \end{cases}. \tag{6}$$

According to formula (6), it is not possible to determine the deformation of the peripheral areas of a defined rectangle as it cannot be determined for dots less than *m* columns or rows from the edge. The values of obtained deformations are expressed in millimeters and depend on the local base *B* value defined as the difference of *x* or *y* coordinate of points separated by *2m* grid positions:

$$\begin{cases} B_x(k, l) = x(k + m, l, 1) - x(k - m, l, 1) \\ B_y(k, l) = y(k, l + m, 1) - y(k, l - m, 1) \end{cases}. \tag{7}$$

To make the deformation values independent of the measurement base, local relative deformations expressed as dimensionless quantities (usually given in%) are defined as follows:

$$\begin{cases} \varepsilon_x(k, l, n) = \dfrac{\Delta x(k, l, n)}{B_x(k, l)} \\ \varepsilon_y(k, l, n) = \dfrac{\Delta y(k, l, n)}{B_y(k, l)} \end{cases}. \tag{8}$$

On the basis of local deformations, mean values of deformations $S_x(n)$ i $S_y(n)$ on the entire surface of the sample are determined for each image recorded in the measurement process.

Using the results of deformation measurements, it is possible to determine the average value of the Poisson's ratio in the examined area of the paper:

$$v(n) = -\frac{S_x(n)}{S_y(n)}. \tag{9}$$

The obtained value of Poisson's ratio is a function of n – it characterises the state of the material at the time of image recording. In addition, in measurements recorded near the fixed jaw one can analyse the sample sliding out of the jaw by measuring the average value of the *y* coordinate increase of the bottom row of dots.

2.4. Verification of developed technique – assessment of measurement errors

In order to verify the correctness of the developed paper deformation measurement technique, a series of tests was carried out using sequences of images obtained by artificially deforming the real image of an exemplary paper sample, similarly to [10]. It allowed to avoid the influence of image registration errors resulting from possible distortions introduced by the camera optics. Moreover, the actual deformation parameters are known for the generated image sequences. For this purpose, a procedure was developed that generates a series of images gradually deformed by introducing an affine transformation of the original image of the paper sample. The following algorithm was used so that the transformation process would not introduce unwanted image distortions:

1) reading the source image from a file,
2) scaling the image enlarging it 50 times,
3) generating image sequence by repeating the following operations for each image:
   - find new values of the elements of image affine transformation matrix,
   - apply affine transformation to the enlarged image,
   - reduce the resulting image size by a factor of 50,
   - save the image as an uncompressed image file.

The following image sequences were generated to evaluate displacement tracking accuracy:
1) translation in the vertical direction by 2 pixels,
2) translation at a given angle to the vertical direction by 15 pixels,
3) image rotation by 2 degrees,
4) scaling the image in one dimension by 3% (simulation of unidirectional distortion)
5) shear (simulation of shear deformation resulting from the action of shear forces) deformation to the level $\tan(\theta) = 0.03$.

The small values of the generated displacements were deliberately used to assess the correctness of determining movement in the image with sub-pixel accuracy. The choice of the range of rotation and shear was dictated by the occurrence of this type of phenomena in actual measurements of paper deformation at a level not exceeding these values. The generated image sequences were analysed with a marker tracking procedure developed by the authors. Thus, the movement of markers estimated by the procedure was compared with the predicted movement obtained by the affine transformation of marker coordinates. The error of each marker displacement was determined for each image in the test sequence, determined which allowed to calculate the standard deviation of the marker displacement from the assumed movement model. Table 1 summarizes mean values of standard deviation of the marker movement and its maximum values over the entire image sequence. The obtained accuracy of displacement estimation in purely translational movement is comparable to the accuracy obtained with the GeoPIV-RG algorithm. It can be surprising because GeoPIV-RG implements tracking refinement on the basis of estimating the quality of matching local image areas. The authors' algorithm lacks this step, but similar results can be explained by the limitation to tracking only markers clearly visible in the image, strongly contrasting with the rest of the sample surface. Tracking them by fitting the dot model by means of linear filtering gives a reliable estimate of their position with an average accuracy of 0.0025 pixels.

The error rate increases by about 20% when there is simultaneous movement in two directions and by 30% when there is pure rotation. Worse results were obtained for subjecting the image to distortions corresponding to the stretching of the paper sample and the shearing deformation of the paper. This can be explained by less reliable tracking of distorted markers. Next, errors of deformation measurements were estimated for a real image sequence. The grid of dots was printed

Table 1. Standard deviation of the marker movement determined from the motion model used in synthesised test sequences.

Type of image transformation	Vertical translation	Translation at a given angle	Image rotation	Scaling in one direction	Shear transformation
Average value of the standard deviation of the marker movement in the horizontal direction, px	0.0019	0.0026	0.0030	0.0187	0.0244
Average value of the standard deviation of the marker movement in the vertical direction, px	0.0021	0.0024	0.0025	0.0367	0.0236
Maximum value of the standard deviation of the marker movement in the horizontal direction, px	0.0044	0.0040	0.0056	0.0361	0.0483
Maximum value of the standard deviation of the marker movement in the vertical direction, px	0.0037	0.0049	0.0039	0.0707	0.0453

on a rigid plate, and it was fixed in the movable jaw of a testing machine. The displacement of the rigid plate was measured in this procedure. Lack of deformation of the plate allowed for estimating the errors of the measurement method. Since the plate is a rigid object, the displacement vector of all dots should be the same and no deformation should be observed. Non-zero deformation values, *i.e.* differences in displacement values of individual points were treated as a measurement error. The standard deviation of individual marker motion observed during plate movement was determined. The standard deviation of this motion was 0.21 μm. This allows to evaluate the error of the developed measurement technique resulting from image acquisition conditions, sensor noise, image discretization and dot tracking methods with a 95% confidence level at 0.42 μm. Comparing this value to the distance of 5.73 μm between pixels in the image sensor, gives an accuracy of 0.07 pixel.

2.5. Synchronization of displacements recorded by the testing machine and measured using the image analysis – based method

To be able to associate the measurement data obtained from the testing machine and the results of the image analysis, it is necessary to synchronize them in time. In order to simultaneously compensate for errors resulting from apparent motion of the immovable jaw and synchronize the sequence of photos with the measurement made with the use of the testing machine, the simultaneous recording of images of three objects was used: a plate with the printed chessboard connected rigidly with the still jaw, a plate connected rigidly with the movable jaw, and a sample of paper subjected to stretching (Fig. 4a). Based on the image data, the displacement of the plate associated with the movable jaw was determined in subsequent images during the measurement. Data synchronization consisted in correcting the initial value of the image capture time by Δt to minimize differences in the movable jaw movement as a function of time, determined from image data and read from the testing machine. An example of the synchronization effect is shown in Fig. 4b.
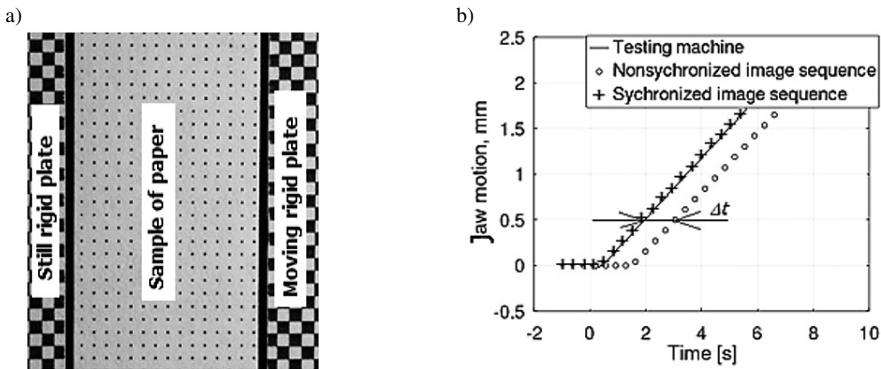
Fig. 4. a) Image of the tested paper sample and plates connected with the jaws, b) the effect of measurement data synchronization.

3. Examples of applications of optical deformation measurement

The developed measurement technique was applied to measuring deformations of packaging paper with grammage of 150 g/m^2 and thickness of 0.22 mm. This type of paper contains very small amounts of additives, which makes it porous. The paper to be tested was pre-prepared by printing a grid of black dots 1 mm apart from each other and cut into 15 mm wide strips. Before the test, the samples were dried and air-conditioned in air with a relative humidity of 50% and temperature of 23°. The tensile test was performed at a constant speed of 20 mm/min with sample attachment length of 180 mm (PN-EN ISO 1924-2:2010 standard) [1]. An initial force of 5N was used to strain the sample of paper. Strain analysis was performed in the region located in the middle of the sample length including 14 columns of dots in the direction of stretching and 30 rows of dots in direction to the stretching direction. The length of the base B on which deformations were determined was 4 mm. Further, the stretching direction will be marked as y, and the direction perpendicular to it in the paper plane as x. The results of measurements of paper deformations are presented in Figs. 5 and 6. Figure 5 presents graphs of selected relative deformation profiles of packaging paper as a function of distance from the bottom edge of the analysed sample fragment, in the direction of stretching and in the direction perpendicular to the direction of stretching, respectively. Subplots a) and b) show deformations of paper stretched in MD. Subplots c) and d) show deformations of paper stretched in a direction perpendicular to the MD, referred to as CD.

Having strains in the direction of stretching and perpendicular to it, Poisson's ratio was calculated for the range of strains of not less than 30% of the breaking strain (Fig. 6).

The limitation of the range of deformations was due to the large value of Poisson's ratio estimation errors at the beginning of the measurement when the relative deformations are still small. Figure 6 shows the relationship between the Poisson's ratio and the average relative deformation of the tested paper sample. The linear approximation of the curves in the diagrams allows to estimate the value of the Poisson's ratio for very small deformations. The obtained values of the coefficient are consistent with the literature data [21]. The results of the measurements confirm the reports known from the literature [19, 20] about the very large heterogeneity of local deformations of fibrous structure subjected to unidirectional tensile load acting in the paper plane. Based on the values of strain in the direction of stretching and perpendicular to stretching at different levels of average strain, its effect on the value of the Poisson's ratio can be analysed. This
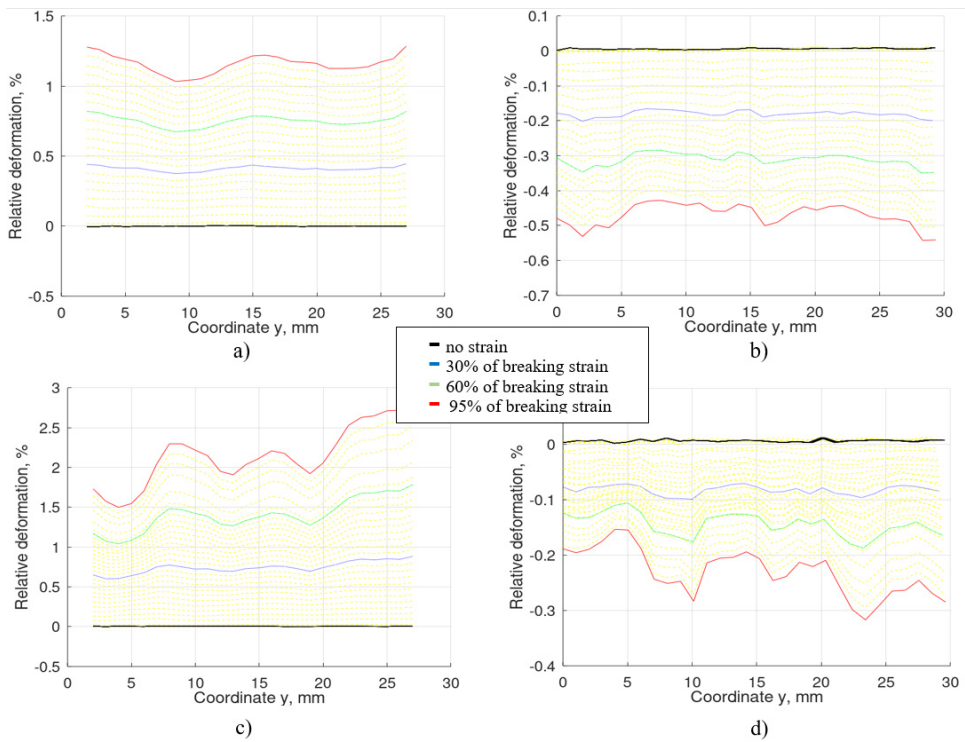
Fig. 5. Relative deformation profiles a) in the stretching direction, b) perpendicular to the stretching direction of packaging paper stretched in the MD direction, c) in the stretching direction, d) perpendicular to the stretching direction of packaging paper stretched in the CD.
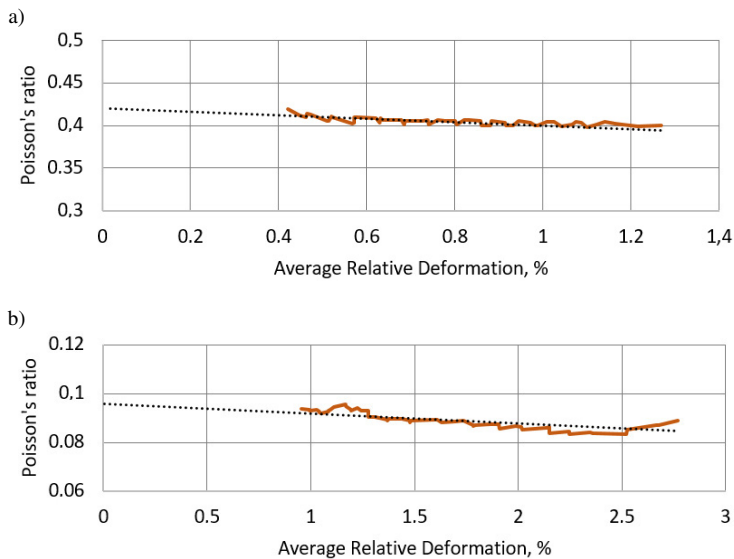

Fig. 6. Dependence of Poisson's ratio on average relative deformation of the tested packaging paper sample a) stretched in the MD, b) stretched in the CD.

is an advantage of the method, while its disadvantage is the inability to investigate the Poisson's ratio in the range of small deformations of up to 30% as opposed to the method based on the measurement of propagation velocity of the ultrasonic wave in a paper sample [18, 20].

4. Conclusions

The optical technique of measuring paper deformation presented in the paper allows registration of deformations of a stretched paper sample in any direction on its plane. Thanks to this, it can be used to test its various properties determined on the basis of a unidirectional tensile test. In particular, it allows for testing deformations in a direction perpendicular to the stretching direction which is not possible when using typical automatic testing machines that do not have optical extensometers. The technique can be easily applied owing to the use of photographic devices and equipment commonly available on the market. Despite the use of a camera and a lens with very good parameters, the solution turned out to be cheaper than using dedicated cameras, which are much more expensive due to the much smaller scale of production [14, 15]. Simultaneous recording of the image of a stretched paper sample and rigid plates with a chessboard pattern associated with the fixed and movable jaw of the testing machine allowed for compensation of small image displacements resulting from lack of a rigid connection of the camera with the machine and synchronization of the measurement time of photos with measurements made using the machine. Thanks to this, there was no need to use expensive data acquisition systems to record measurement data simultaneously with image capturing. Additionally, by using a square dot print on the tested paper, it was possible to find the parameters of the camera position relative to the sample which allowed for compensation of errors resulting from the projection of points of the tested material on the image sensor. An important advantage of the developed technique is that it allows simultaneous tracking of deformations of very small areas distributed over the entire tested surface of the sample, and thus the variability of local strains as a function of the mean strain value in the direction of stretching. By synchronizing the strains determined using this method with the strains recorded by the testing machine, it is possible to link the mean and local strains to the load that causes them. Another advantage of the method over the classic ones in which large samples were used is lack of problems resulting from transverse creasing of the stretched paper, which falsely increases the value of deformation in a direction perpendicular to the direction of stretching. Thus, when determining the value of Poisson's ratio, there is no need to use devices maintaining flatness of the tested sample [20, 21]. The disadvantage of the developed technique is that it is limited to papers with smooth, bright surface. The presence of the fibres of low brightness causes them to be incorrectly detected as dots in the printed pattern and may cause errors in estimating deformations. To overcome this limitation in the future, it is planned to develop a deformation analysis technique based on digital correlation of the image with printed, regular grid of markers. This will increase the resolution of deformation measurements in the case of textured surface while minimizing the interference of toner applied to the paper on its physical properties.

References

[1] Polish Committee for Standardization. (2010). *Paper and cardboard – Determination of tensile properties – Part 2: Test at constant tensile speed (20 mm / min)* (ISO Standard No. PN-EN ISO 1924-2). (in Polish)

[2] Laermann, K. H. (Eds.). (2000). *Optical Methods in Experimental Solid Mechanics*. Springer. https://doi.org/10.1007/978-3-7091-2586-1

[3] Zhu, C., Wang, H., Kaufmann, K., & Vecchio, K. S. (2020). A computer vision approach to study surface deformation of materials. *Measurement Science and Technology*, *31*(5), 055602. https://doi.org/10.1088/1361-6501/ab65d9

[4] Sutton, M. A. (2008). Digital Image Correlation for Shape and Deformation Measurements. In: Sharpe, W. (Eds.). *Springer Handbook of Experimental Solid Mechanics*. *Springer Handbooks* (pp. 565-600). Springer. https://doi.org/10.1007/978-0-387-30877-7_20

[5] Sutton, M. A., Orteu, J. J., & Schreier, H. (2009). *Image correlation for shape, motion and deformation measurements: basic concepts, theory and applications*. Springer Science & Business Media. https://doi.org/10.1007/978-0-387-78747-3

[6] Khoo, S. W., Karuppanan, S., & Tan, C. S. (2016). A review of surface deformation and strain measurement using two-dimensional digital image correlation. *Metrology and Measurement Systems*, *23*(3), pp. 461–480. https://doi.org/10.1515/mms-2016-0028

[7] Debella-Gilo, M., & Kääb, A. (2010). Sub-pixel Precision Image Matching for Displacement Measurement of Mass Movements Using Normalised Cross-Correlation. *ISPRS TC VII Symposium – 100 Years ISPRS*, Austria, *XXXVIII*, Part 7B.

[8] White, D. J., Take, W. A., & Bolton, M. D. (2003). Soil deformation measurement using particle image velocimetry (PIV) and photogrammetry. *Geotechnique*, *53*(7), 619–631. https://doi.org/10.1680/geot.2003.53.7.619

[9] Take, W. A. (2015). Thirty-Sixth Canadian Geotechnical Colloquium: Advances in visualization of geotechnical processes through digital image correlation. *Canadian Geotechnical Journal*, *52*(9), 1199–1220. https://doi.org/10.1139/cgj-2014-0080

[10] Stanier, S. A., Blaber, J., Take, W. A., & White, D. J. (2016). Improved image-based deformation measurement for geotechnical applications. *Canadian Geotechnical Journal*, *53*(5), 727–739. https://doi.org/10.1139/cgj-2015-0253

[11] Chivers, K. & Clocksin, W. (2000). Inspection of Surface Strain in Materials Using Optical Flow, In Mirmehdi, M. & Barry T., (Eds.). *Proceedings of the British Machine Conference*. BMVA Press. https://doi.org/10.5244/C.14.41

[12] Lyubutin, P. S. (2015). Development of optical flow computation algorithms for strain measurement of solids. *Computer Optics*, *39*(1), 94–100. https://doi.org/10.18287/0134-2452-2015-39-1-94-100

[13] Hartmann, C., & Volk, W. (2019). Digital image correlation and optical flow analysis based on the material texture with application on high-speed deformation measurement in shear cutting. *International Conference on Digital Image & Signal Processing*, United Kingdom.

[14] Jiao, W., Fang, Y., & He, G. (2008). An integrated feature -based method for sub-pixel image matching. The International Archives of the Photogrammetry, China, *XXXVII*, Part B1.

[15] Zwick Roell. *Product Information videoXtens 2-120 HP*. https://www.zwickroell.com

[16] Narita, G., Watanabe, Y., & Ishikawa, M. (2016). Dynamic projection mapping onto deforming non-rigid surface using deformable dot cluster marker. *IEEE Transactions on Visualization and Computer Graphics*, *23*(3), 1235–1248. https://doi.org/10.1109/TVCG.2016.2592910

[17] Mishra, S. R., Mohapatra, S. R., Sudarsanan, N., Rajagopal, K., & Robinson, R. G. (2017). A simple image-based deformation measurement technique in tensile testing of geotextiles. *Geosynthetics International*, *24*(3), 306–320. https://doi.org/10.1680/jgein.17.00003

[18] Duda, A., & Frese, U. (2018). Accurate Detection and Localization of Checkerboard Corners for Calibration. *29th British Machine Vision Conference* (BMVC-29), United Kingdom. https://bmvc2018.org/contents/papers/0508.pdf

[19] Jones, A. R. (1968). An Experimental Investigation of the In-Plane Elastic Moduli of Paper. *Tappi*, *51*(5), 203–209.

[20] Szewczyk, W. (2008). New methods of assessing the load capacity of multilayer laminates of paper and cardboard. *Science Notebooks Lodz University of Technology*, 1027. (in Polish).

[21] Cao, X., Bi, Z., Wei, X., & Xie, Y. (2012). Determination of Poisson's Ratio of Kraft Paper Using Digital Image Correlation. In: Zhang T. (Eds.). *Mechanical Engineering and Technology*. *Advances in Intelligent and Soft Computing* (pp. 51-57), *125*. Springer. https://doi.org/10.1007/978-3-642-27329-2_8

Paweł Pełczyński received the Ph.D. degree from Lodz University of Technology, Poland, in 2003. He is currently employed in the Centre of Papermaking and Printing, Lodz University of Technology. He has authored or co-authored, over 25 journal and 20 conference publications. He holds 2 issued patents. His current research focuses on image-based measurement methods and their applications for testing paper products.

Włodzimierz Szewczyk received the Ph.D. degree from Lodz University of Technology, Poland, in 1997. He is currently the Vice Director of the Development Centre of Papermaking and Printing, Lodz University of Technology. He has authored or coauthored 2 books and over 50 journal publications. He holds 6 issued patents. His research activity focuses on researching the strength properties of papers, cardboard and products made of them.

Maria Bieńkowska obtained her M.Sc. degree in printing technology from Lodz University of Technology, Poland in 2009. She is currently working on her doctoral dissertation. Her resarch activity focuses on mechanical properties of papers, corrugated cardboards and packagings.